PNAS RESEARCH ARTICLE | DEVELOPMENTAL BIOLOGY OPEN ACCESS

# Lateral cell polarization drives organization of epithelia in sea anemone embryos and embryonic cell aggregates

Tavus Atajanova[a,1], Emily Minju Kang[a,1], Anna Postnikova[a,1], Alivia Lee Price[a], Sophia Doerr[a], Michael Du[a], Alicia Ugenti[a], and Katerina Ragkousi[a,2]

Edited by John Gerhart, University of California, Berkeley, CA; received May 2, 2024; accepted September 19, 2024

**One of the first organizing processes during animal development is the assembly of embryonic cells into epithelia. Common features unite epithelialization across select bilaterians, however, we know less about the molecular and cellular mechanisms that drive epithelial emergence in early branching nonbilaterians. In sea anemones, epithelia emerge both during embryonic development and after cell aggregation of dissociated tissues. Although adhesion is required to keep cells together, it is not clear whether cell polarization plays a role as epithelia emerge from disordered aggregates. Here, we use the embryos of the sea anemone *Nematostella vectensis* to investigate the evolutionary origins of epithelial development. We demonstrate that lateral cell polarization is essential for epithelial organization in both embryos and aggregates. With disrupted lateral polarization, cell contact in the aggregate is not sufficient to trigger epithelialization and further tissue development. Specifically, knockdown of the conserved lateral polarity and tumor suppressor protein Lethal giant larvae (Lgl) disrupts epithelia in developing embryos and impairs the capacity of dissociated cells to epithelialize from aggregates. In contrast to other systems, cells in *Nematostella lgl* knockdown embryos do not undergo excessive proliferation. Cells with reduced Lgl levels lose their columnar shape and proper positioning of their mitotic spindles and basal bodies. Due to misoriented divisions and aberrant shapes, cells arrange nonuniformly without forming a monolayer. Together our data show that, in *Nematostella,* Lgl drives epithelialization in embryos and cell aggregates through its effect on cell shape and organelle localization.**

epithelia | lateral polarity | aggregate | *lethal giant larvae* | *Nematostella vectensis*

## Significance

Cells from dissociated embryos of the sea anemone *Nematostella vectensis* organize into animals after reaggregation. The first mark of organization is the emergence of epithelia, and that has been attributed to successful cell adhesion upon contact. We found that dissociated cells from embryos with disrupted polarity fail to organize into epithelia by contact alone. The establishment of lateral polarity aids cell organization into columnar epithelia. Disruption of lateral polarity alters cell shape and the position of spindle poles and basal bodies. This mispositioning of intracellular organelles interferes with oriented divisions and cell arrangement within the monolayer. Thus, in aggregates and embryos, epithelialization relies on the capacity of cells to polarize their lateral interfaces and couple their intracellular organization to tissue-level order.

Epithelia emerge as polarized layers of interconnected cells in a highly divergent and context-dependent manner across all animals (1, 2). However, the prevailing hypothesis is that common principles underly metazoan epithelialization, and these can be traced to early branching animals including sponges and cnidarians (1, 3–5). Many studies in bilaterian animals (*Drosophila*, mouse, nematodes) have discovered conserved epithelial genes and placed them in a unifying model to broadly explain epithelial organization (2, 6). We are still missing molecular and cellular information on how nonbilaterian epithelia emerge. Genomic studies have identified conserved orthologs of epithelial genes in cnidarians and recent functional analyses have started to address their role in epithelial organization (7–10). However, open questions on the emergence of primary epithelia in nonbilaterian species remain.

The cnidarian *Nematostella vectensis* is a sea anemone and provides an excellent system to investigate the ancestral mechanisms of epithelialization as *Nematostella* epithelia emerge from both embryos and aggregates of dissociated tissues (11, 12). During embryonic development, epithelia emerge as cells connect via lateral adhesions and differentially pattern their two opposing domains; the apical domain develops at the interface with the extracellular environment or lumen and the basal domain develops where the monolayer faces adjacent tissues or the basal membrane (2, 6). Remarkably, epithelia also emerge from reaggregated cells of dissociated tissues as a first step toward rebuilding the animal body. Such whole-body reconstitution begins with the sorting and organization of reaggregated cells into inner and outer epithelia (12–17). Studies in other experimental systems pointed to differential adhesion and tension as powerful drivers of cell sorting into distinct compartments (18, 19). However, it is not clear how dissociated cells organize into epithelia in the first place. It is also not clear whether embryonic and aggregate epithelialization rely on similar molecular mechanisms. Although intercellular adhesion is essential, whether cell polarity plays a role in this process remains unknown.

*Nematostella* embryos assemble into polarized monolayers by the 16-cell stage (11, 20). Similar to other epithelia, polarization of embryonic cells becomes evident with the differential localization of proteins in the apical and lateral domains. Conserved cadherin–catenin

Author affiliations: [a]Department of Biology, Amherst College, Amherst, MA 01002

Author contributions: K.R. designed research; T.A., E.M.K., A.P., A.L.P., S.D., M.D., and K.R. performed research; A.U. contributed new reagents/analytic tools; T.A., E.M.K., A.P., S.D., and K.R. analyzed data; and T.A., E.M.K., A.P., S.D., and K.R. wrote the paper.

The authors declare no competing interest.

This article is a PNAS Direct Submission.



[1]T.A., E.M.K. and A.P. contributed equally to this work.

[2]To whom correspondence may be addressed. Email: kragkousi@amherst.edu.

This article contains supporting information online at https://www.pnas.org/lookup/suppl/doi:10.1073/pnas.2408763121/-/DCSupplemental.

Published October 29, 2024.

complexes in the apical junctions keep cells together and polarity proteins localize to their apical (Par6 and aPKC), junctional (Par3), and lateral (Par1 and Lgl) domains (9, 10, 20, 21). We asked whether cell polarity is essential for *Nematostella* aggregate and embryonic epithelialization. We found that organization of lateral polarity is crucial for epithelialization in both embryos and aggregates. Knocking down the lateral polarity protein Lethal giant larvae (Lgl) impaired the formation of outer epithelia in aggregates. In embryonic epithelia, *lgl* knockdown disrupted cell shape and orientation of cell cleavages. Strikingly, *lgl* knockdown epithelia exhibited a dramatic mispositioning of their ciliary basal bodies. Interestingly, Lgl was originally discovered in *Drosophila* and was shown to function as a tumor suppressor by regulating both epithelial organization and cell proliferation (22, 23). In the absence of an obvious effect on cell proliferation, our combined results indicate that, in *Nematostella,* Lgl helps organize embryonic and aggregate epithelia as a cytoskeletal regulator. Our data also demonstrate that without lateral polarization, cell contact is not sufficient to drive de novo epithelialization and further tissue development. Thus, lateral polarization via the function of Lgl hints at an ancestral mechanism that drives cell organization in metazoan epithelia.

## Results

**The Lateral Polarity Protein Lgl Is Essential for Epithelialization of *Nematostella* Embryonic Cell Aggregates.** Self-organization of tissues from aggregated cells begins with the emergence of epithelial layers. *Nematostella* aggregates form a smooth layer around their colony within 6 to 12 h post dissociation (hpd). By 24hpd, outer (ectodermal) and inner (endodermal) layers are defined in structure and fate identity (12).

We sought to examine whether polarity proteins are important for de novo epithelialization of aggregates from dissociated embryonic cells. During early *Nematostella* development, the well-conserved structural protein Par6 localizes with the atypical kinase aPKC at the apical cortex and marks together with Par3 the apical cell junctions, while Lgl is enriched along the lateral cell contacts (20, 21). Among the three polarity proteins previously tested, Lgl is expressed the highest during early development, approximately 30 times the levels of each of Par3 and Par6 (8). We hypothesized that the continuous expression of *lgl* is required for the epithelialization of both embryos and cell aggregates. Importantly, in the event where dissociated cells lack a critical epithelialization protein, aggregates will fail to organize and eventually fall apart. To this end, we tested two separate short RNA hairpins that knock down the expression of *lgl* in *Nematostella* embryos and then dissociated the embryos and reaggregated their dissociated cells into a solid cell mass as previously described (Fig. 1*A*) (12). We then examined the aggregates in two ways: 1) by recording aggregate behavior by live time-lapse imaging (*SI Appendix*, Fig. S1, Movies S1-S3) and 2) by fixing aggregates at 0hpd and at 24hpd, staining for F-actin and DNA, and visualizing by confocal microscopy (Fig. 1*B* and *SI Appendix*, Fig. S2*A*).

Live observation of aggregates by time-lapse imaging showed that aggregates from sh*gfp* control embryos all organized into compact cell assemblies, while aggregates from sh1*lgl* and sh2*lgl* embryos failed to compact (*SI Appendix*, Fig. S1 and Movies S1–S3). Interestingly, epithelialization differences across aggregates appeared as early as 5.5hpd; a critical time point by which ectodermal epithelia become apparent (12). By 11hpd, sh1*lgl* aggregates disintegrated into progressively smaller fragments that remained separate by the end of imaging (22hpd) (*SI Appendix*, Fig. S1 and Movie S2).

Confocal imaging of fixed aggregates confirmed and expanded upon the live imaging observations. Aggregates from control

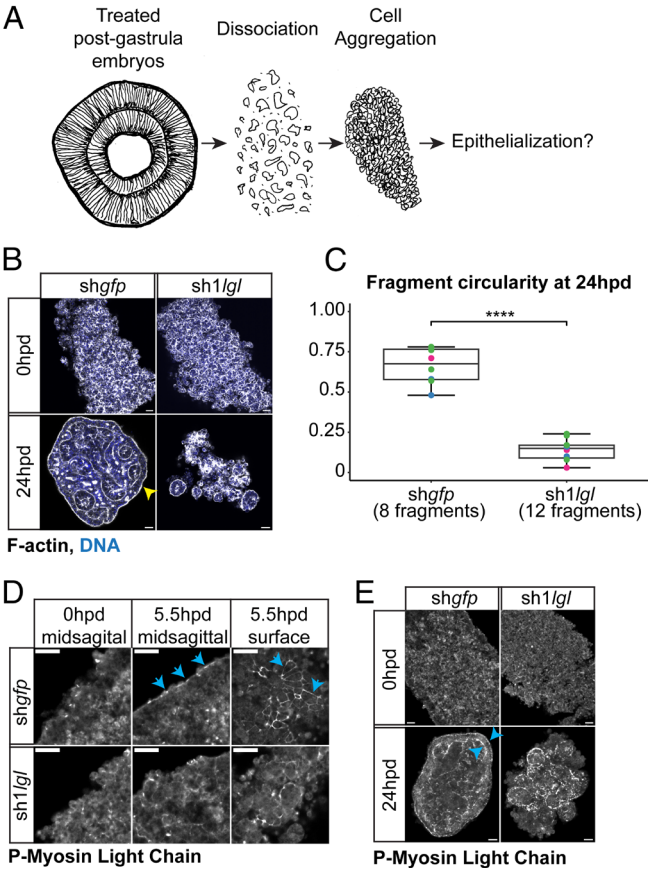


**Fig. 1.** The lateral polarity protein Lgl is essential for epithelialization of *Nematostella* embryonic aggregates. (*A*) Schematic of the experimental process starting with embryo dissociation and aggregate formation as described in ref. 12 (*B*) Aggregate formation from dissociated sh*gfp* (control) and sh1*lgl* embryos at the time of aggregation (0hpd) and 24hpd. Epithelialization is complete by 24hpd with the organization of cells into a common aggregate with an outer polarized layer and organized internal layers. Yellow arrowhead points to the outer layer of the sh*gfp* aggregate which is absent from the sh1*lgl* aggregate. Cells from dissociated sh1*lgl* embryos fail to organize into a common epithelial aggregate and small cell clusters eventually disintegrate. Similarly, aggregates from sh2*lgl* embryos show no obvious enveloping epithelial layer, although more cells remain in contact (*SI Appendix*, Figs. S1 and S2). (*C*) As the aggregate organizes within the enveloping layer, it acquires a compact shape quantified by the extent of its circularity. Shape quantification of aggregates at 24hpd acquire circularity >0.5 for the majority of sh*gfp* and <0.3 for sh1*lgl* aggregates, indicating failure of sh1*lgl* cells to compact within a common layer. Colors blue, green, and magenta correspond to three independent experiments (ANOVA; ****$P < 0.0001$). (*D*) Blue arrows point to phosphorylated myosin light chain (PMLC) enriched at apical junctions of cells undergoing epithelialization at the periphery of the aggregate at 5.5hpd. (*E*) By 24hpd, PMLC marks both the apical and basal junctions of the outer layer in sh*gfp* aggregates. In sh*lgl* aggregates, PMLC is instead enriched at the cortex of 5.5hpd rosette-like cell clusters which remain distinct and separate by 24hpd. Images show midsagittal sections unless otherwise stated. One of four aggregates is shown from one of three independent experiments. The largest 24hpd sh1*lgl* aggregate of all samples is shown. (Scale bars, 20 μm.) See also *SI Appendix*, Figs. S1 and S2 and Movies S1–S3.

embryos electroporated with sh*gfp* alone developed a continuous and smooth epithelial monolayer encompassing internally organized cell layers indicating the formation of both ectodermal and endodermal territories. In contrast, aggregates from both sh1*lgl* and sh2*lgl* embryos lacked an enveloping layer. Notably, fewer sh1*lgl* cells maintained their adhesions (Fig. 1*B* and *SI Appendix*, Fig. S2*A*). In contrast to sh*gfp*, both sh1*lgl* and sh2*lgl* aggregates thinned into small clusters that disintegrated and did not give rise to a living animal 7 d post dissociation. We further quantified the extent of epithelialization by determining the shapes of the aggregates at 24hpd. As the aggregate acquires its outer layer, cells are organized into a compact structure that resembles an

almost-spherical embryo with circularity values approaching that of the perfect circle (circularity =1). We found that sh*gfp* aggregates had high circularity values (circularity > 0.5), while both sh1*lgl* and sh2*lgl* aggregates had very low circularity values (circularity < 0.3) due to the absence of an outer organizing epithelium (Fig. 1*C* and *SI Appendix*, Fig. S2*B*).

In addition to their shape, we examined aggregates for the presence of adherens junctions between their cells as an additional hallmark of epithelialization. The phosphorylated version of myosin light chain (PMLC) localizes to contractile adherens junctions (24). By 5.5hpd, some cells near the surface of the sh*gfp* aggregate had enriched PMLC at their apical junctions (Fig. 1*D*). By 24hpd, PMLC localization expanded to the basal cell junctions of the outer layer that enveloped the sh*gfp* aggregate (Fig. 1*E*). In sh1*lgl* aggregates, PMLC localized at the cortex of cells arranged in rosette-like clusters which became more prominent by 24hpd (Fig. 1 *D*-*E*). While sh*gfp* cells organized outer and inner epithelia within the enveloped aggregate, sh1*lgl* cells remained in rosette-like clusters and failed to integrate within a common assembly defined by an outer layer.

We conclude that in the absence of continuous *lgl* expression, single cells from dissociated embryos fail to organize into viable epithelial aggregates. Although sh*lgl* cells come into direct contact, their assembly does not progress past their initial clustering and fails to organize within a common outer layer.

**Expression of *lgl* Is Essential for Epithelial Organization of Developing *Nematostella* Embryos.** We reasoned that the lack of epithelialization in sh*lgl* aggregates may be traced back to the compromised epithelial integrity of knockdown embryos. In the absence of *lgl* expression, embryos appeared to develop and gastrulate normally (Fig. 2 *A* and *B*). However, on closer inspection of *lgl* knockdown embryos stained with FITC-phalloidin to outline cell boundaries, we noticed an unusual number of depressions in the ectodermal epithelia (Fig. 2 *C*–*E* and *SI Appendix*, Fig. S2 *C*–*E*). While mitotic round cells are normally restricted in the apical domain of the epithelium, in both sh1*lgl* and sh2*lgl* embryos, many nonmitotic round cells were observed in the basal domain (Fig. 2*F* and *SI Appendix*, Fig. S2*F*). At some regions, ectodermal depressions appeared in the vicinity of basally located round or misshapen cells. In a few mildly deformed sh1*lgl* and sh2*lgl* embryos, disorganization appeared in restricted regions of the epithelium (Fig. 2 *C*–*D* and *SI Appendix*, Fig. S2 *C*–*D*). However, the majority of sh*lgl* embryos manifested global epithelial disorganization with basal round cells and more ectodermal depressions compared to controls. In some severely damaged embryos, cells appeared to undergo lysis. However, these embryos also appeared in similar numbers in the control group (sh*gfp*), and we reasoned that this is not due to specific hairpin knockdown effects.

Taken together, our data suggest that expression of Lgl is essential for both de novo epithelialization of cell aggregates and epithelial organization of embryos.

**Basal Domains are Disorganized in *lgl* Knockdown Epithelia.** We then sought to determine the mechanism by which knockdown of *lgl* disrupts epithelia. Lgl is enriched at the lateral cell contacts in *Nematostella* embryos (20, 21). In epithelia of other species, Lgl restricts the localization of apical polarity proteins to the apical domain (2, 6, 25). Reduced Lgl levels are likely to disrupt epithelia by impairing cell polarity. To examine cell polarity in *Nematostella* embryos, we checked the localization of conserved proteins known to localize to the apical and basal domains in epithelial cells. We first examined whether apical domains are properly patterned in *lgl* knockdown epithelia by checking the localization of Par3-GFP and Par6-GFP. In both sh*mcherry* controls and sh1*lgl* embryos, Par6-GFP was enriched at the apical cortices and apical cell junctions (Fig. 2*G*). Similarly, Par3-GFP was found at the apical cell junctions of both control and sh1*lgl* embryos (*SI Appendix*, Fig. S3). However, in contrast to controls, some cells in *lgl* knockdown embryos had Par6-GFP and Par3-GFP enriched at their basal domains as well (Fig. 2*G* and *SI Appendix*, Fig. S3).

Enrichment of apical proteins in basal epithelial regions suggests a basal polarization defect. We further examined the integrity of basal domains by visualizing the localization of a GFP fusion to the junction protein α-catenin. *Nematostella* ectodermal epithelia are unique in that junctional Cadherin3 is enriched in both apical and basal domains (9). Similar to Cadherin3 localization, we found α-catenin-GFP enriched at both apical and basal cell junctions of wild-type epithelia (Fig. 2*H*). However, in *lgl* knockdowns, α-catenin-GFP was not consistently found in the basal domain of the ectodermal monolayer and was instead distributed at shorter distances from the apical domain (Fig. 2 *H*–*I*). This could be due to basal domains established at shorter cell lengths along the *lgl* knockdown epithelium. Alternatively, α-catenin-GFP could be mis-localized along the cell periphery instead of a defined basal domain. In either case, mis-localization of α-catenin-GFP points to disorganized basal junctions when *lgl* is knocked down. Indeed, the phosphorylated myosin (PMLC) that is enriched at defined junctions in control epithelia was also found to be disorganized and was distributed at various lengths along the *lgl* knockdown monolayer (Fig. 2*J*).

Taken together, examination of polarity and junction protein localization demonstrates that basal domains are disorganized in *lgl* knockdown epithelia. The basal junctional markers, α-catenin-GFP and PMLC, appear enriched in shorter distance from the apical domain. These mispositioned basal junctions, if still functional, likely alter the contractile properties and behaviors of both individual cells and the ectodermal epithelium at large.

**Epithelial Disorganization in *lgl* Knockdown Embryos Is not due to Uncontrolled Cell Proliferation.** Since its discovery as a tumor suppressor in the fly, Lgl has been implicated in both epithelial organization and cell proliferation (22, 23). The *lgl* mutations transform the fly imaginal discs into lethal neoplasms and the optic primordia of the brain into neuroblastoma (22, 26). Later work showed how Lgl together with Scribbled and Dlg, regulates cell polarity and epithelial organization in various fly epithelia (23). Similarly, knockout of one of the two Lgl homologs in mice (Lgl1) gives rise to disorganized neuroepithelial structures similar to human neuroectodermal tumors (27). Thus, we hypothesized that the epithelial disorganization observed in our *Nematostella* sh*lgl* knockdown embryos is attributed to cell over proliferation. We reasoned that due to the high variability of embryo size during development and the effect of *lgl* knockdown on embryo shape, quantification of embryo size does not precisely capture cell over proliferation (11, 20). Therefore, to examine whether cell proliferation control is disrupted, we fixed sh*gfp* control and sh1*lgl* embryos at different stages during development and counted all stained nuclei. We also specifically identified mitotic nuclei using a phosphorylated Histone H3 (PH3) antibody and quantified the ratios of mitotic nuclei to total nuclei. Assuming that there is one nucleus per cell, these quantifications reveal that both sh*gfp* and sh1*lgl* embryos are composed of similar cell numbers throughout development (Fig. 3 and *SI Appendix*, Fig. S4). These results further demonstrate that epithelial disorganization in *Nematostella* sh1*lgl* knockdown embryos is not coupled to loss of cell proliferation control.

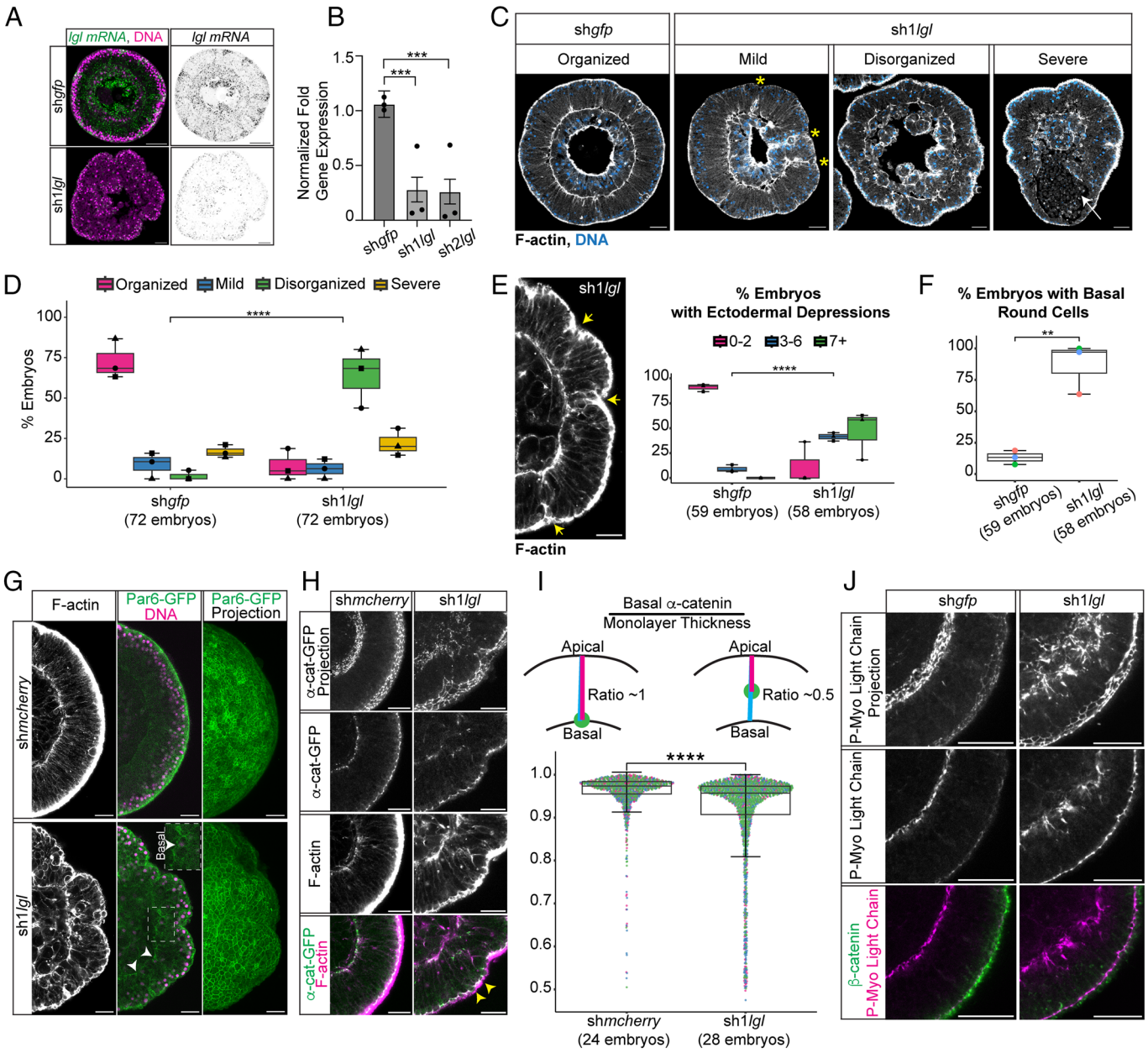


**Fig. 2.** Knockdown of *lgl* disrupts epithelial organization in *Nematostella* embryos. (*A* and *B*) Expression of *lgl* is reduced in postgastrula (28hpf) sh1*lgl* embryos compared to sh*gfp* controls, as verified by in situ hybridization and qPCR of mRNA levels from embryos of three independent experiments. (Wilcoxon rank sum test; ***$P < 0.001$). A separate hairpin, sh2*lgl*, similarly affects *lgl* expression. (*C*) Ectodermal epithelia are disorganized in postgastrula sh1*lgl* embryos and manifest surface depressions not visible in the smooth epithelial layer of sh*gfp* control embryos. (*D*) Quantification of observed phenotypes. "Mild" refers to embryos with epithelial disorganization in restricted areas of the ectoderm, shown near the yellow stars in "mild" embryo of (*A*). "Disorganized" refers to embryos manifesting global epithelial disorganization with obvious depressions and misshapen cells throughout the ectoderm. "Severe" refers to embryos undergoing cell lysis pointed by the white arrow as an obliterated cell mass in "severe" embryo of (*A*). (Fisher's exact test; ****$P < 0.0001$). (*E*) Ectodermal depressions are more frequent in "disorganized" sh1*lgl* embryos and often correspond to areas with basal round cells pointed by the yellow arrows. (Fisher's exact test; ****$P < 0.0001$). (*F*) Basal round cells are prevalent in "disorganized" sh1*lgl* embryos. (ANOVA; **$P = 0.003$). Symbols ■▲● in (*D*) and (*E*), and colors blue, green, and magenta in (*F*) correspond to embryo percentages from three independent experiments. (*G*) Par6-GFP is enriched exclusively at the apical cell cortices and junctions, as shown in the midsagittal and surface projection views of sh*mcherry* control embryos. In sh1*lgl* embryos, Par6-GFP is enriched at apical cell cortices and junctions, similar to controls, as well as some basal regions of the ectodermal epithelium pointed by the white arrowheads. Boxed area shows Par6-GFP localization at the basal domain. (*H*) α-catenin-GFP is enriched at both apical and basal junctions of the ectodermal epithelium. In control sh*mcherry* embryos, apical and basal α-catenin-GFP mark the apical and basal domains of the monolayer at a consistent length along its thickness. In sh1*lgl* embryos, basal α-catenin-GFP is enriched at variable lengths from the apical domain. Projection is the sum of 15 μm above and below the midsagittal section. (*I*) Quantification of basal α-catenin-GFP relative to the monolayer thickness in sh*mcherry* control and sh1*lgl* embryos. Monolayer thickness is determined by F-actin which highlights all cell margins. Ratio = 1 indicates colocalization of basal α-catenin-GFP with the basal domain of the monolayer. Ratio < 1 indicates that basal α-catenin-GFP enrichment does not align along the basal domain and appears within a shorter distance from the apical domain. (Wilcoxon rank sum test; ****$P < 0.0001$). Yellow arrowheads point to a bilayered ectodermal epithelium. (*J*) PMLC is enriched at the apical and basal junctions of the ectodermal epithelium. In sh*gpf* control embryos, PMLC marks the basal domain of the monolayer in a consistent manner along its thickness, similar to the localization of basal α-catenin-GFP. In sh1*lgl* embryos, basal enrichment of phosphorylated myosin is disorganized and appears at variable lengths from the apical domain. Projection is the sum of 8 μm above and below the midsagittal section. All images show midsagittal sections of postgastrula embryos unless otherwise stated. (Scale bars, 20 μm.) See also Par3-GFP localization in *SI Appendix*, Fig. S3.

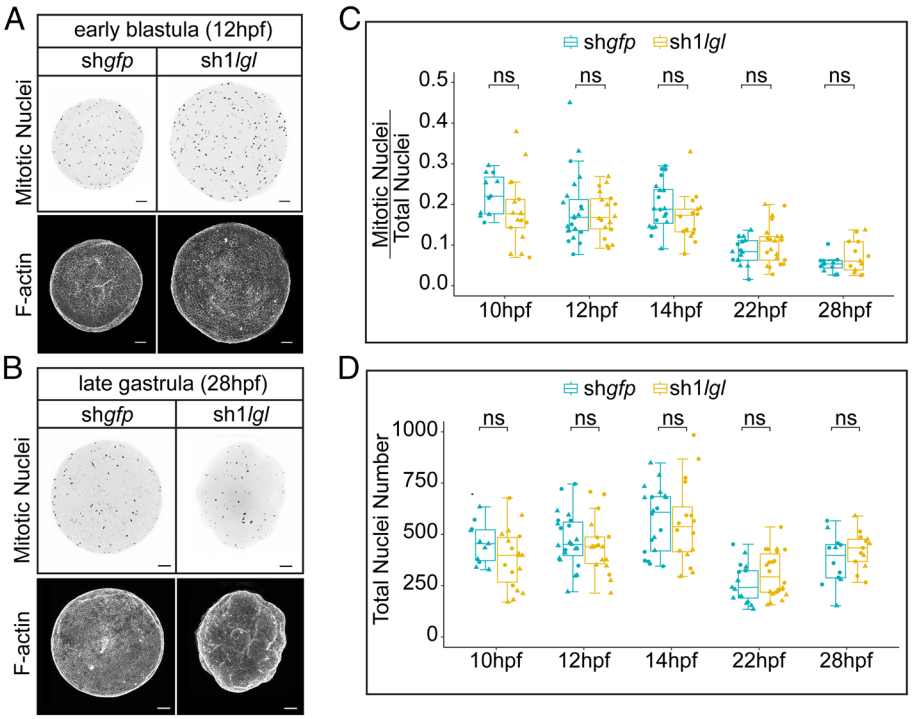


**Fig. 3.** *lgl* knockdown embryos do not exhibit cell over proliferation during development. (*A*) Mitotic nuclei stained with phosphorylated Histone H3 (PH3) antibody and corresponding F-actin-stained sh*gfp* control and sh1*lgl* embryos at: (*A*) early blastula (12hpf) and (*B*) postgastrula (28hpf) stages. (*C*) Quantification of ratios of mitotic nuclei/total nuclei numbers in sh*gfp* control and sh1*lgl* embryos across development. (*D*) Total nuclei quantification in sh*gfp* control and sh*lgl* embryos across development. Symbols ▲● correspond to average values from each embryo analyzed from two independent experiments. Number of sh*gfp* embryos analyzed per time point: 10hpf (11 embryos), 12hpf (23 embryos), 14hpf (20 embryos), 22hpf (17 embryos), and 28hpf (12 embryos). Number of sh1*lgl* embryos analyzed per time point: 10hpf (17 embryos), 12hpf (18 embryos), 14hpf (16 embryos), 22hpf (21 embryos), and 28hpf (13 embryos). (Wilcoxon rank sum test; ns $P > 0.05$). Images show projections of whole embryos. (Scale bars, 20 μm.) See also *SI Appendix*, Fig. S4.

**Lgl Is Required for Planar Spindle Orientation During Early Blastula Cleavages.** Disorganized actomyosin contractility and loss of cortical polarity could explain the appearance of misshapen cells and epithelial depressions in *lgl* knockdown embryos. A direct consequence of disruption in actomyosin and polarity in the epithelium is misoriented cell divisions (28, 29). In epithelia, mitotic spindle orientation is of paramount importance (30–32). To maintain the monolayer structure, spindles must be positioned parallel to the epithelial plane. To examine whether *lgl* knockdown affects spindle orientation in *Nematostella* epithelia, we examined the angle of mitotic spindles relative to the monolayer plane at two early stages, before the epithelial disorganization becomes pronounced (Fig. 4 *A* and *B*). During prophase, we detected high variability of spindle position in both control and *lgl* knockdown embryos independent of their developmental stage. By metaphase, spindles in control embryos appeared to consistently align parallel to the epithelial plane. We did not detect any obvious differences between control (sh*gfp*) and sh1*lgl* spindle orientation during early cleavages (Fig. 4*A*, 6hpf). However, at the blastula stage, when cells in controls are already organized into an epithelial monolayer, *lgl* knockdown significantly impaired spindle orientation (Fig. 4*B*, 12hpf). After this stage, *lgl* knockdown epithelia began to manifest deformities in their structure, impeding precise spindle orientation measurements.

In conclusion, we identified spindle orientation defects in cells of early blastula *lgl* knockdown embryos. These defects could drive cells to undergo oblique or orthogonal divisions relative to the epithelium such that one daughter cell positions its apical "domain" toward the basal domain of the monolayer. Interestingly, we did not identify any Par3-GFP or Par6-GFP enrichment within the ectodermal monolayer. Assuming that daughter cells appear in mirror symmetry relative to each other after orthogonal divisions, the plane of cleavage could explain the appearance of Par3-GFP and Par6-GFP apical proteins in the basal domain of the ectodermal epithelium and basal proteins like α-catenin-GFP and phosphorylated myosin within the epithelium (Fig. 2 *G–J* and *SI Appendix*, Fig. S3). Mispositioned mitotic spindles could lead to the apicobasal polarity defects observed within some regions of the ectodermal epithelium.

**Mispositioning of the Basal Body in *lgl* Knockdown Epithelia.** An unexpected observation in *lgl* knockdown embryos was the mispositioning of ciliary basal bodies. During our examination of epithelial polarity, we serendipitously found that a commercial antibody previously used for β-catenin labeling marked both the apical cell junctions and the basal body of *Nematostella* ectodermal epithelia (*SI Appendix*, Fig. S5). By late blastula stage (18hpf), embryos develop motile cilia and basal bodies become evident at the apical domain of their ectodermal epithelia. Closer inspection revealed that β-catenin localizes in a ring-like pattern around the basal body marked by γ-tubulin near the center of the cell's apical region. Interestingly, in sh1*lgl* knockdown embryos, the basal body was found mispositioned in close proximity to the lateral plasma membrane (Fig. 4 *C* and *D*). We quantified the position of the basal body relative to the nearest cell contact in cells from sh*gfp* control and sh1*lgl* knockdown embryos by using both β-catenin and γ-tubulin markers. We found a significantly higher distribution of basal bodies near the cell contact in sh1*lgl* knockdown epithelia compared to controls (Fig. 4 *E* and *F*). Considering that the basal body is an apically docked cell organelle and apical polarity appeared normal in *lgl* knockdown epithelia, its mispositioning is particularly intriguing.

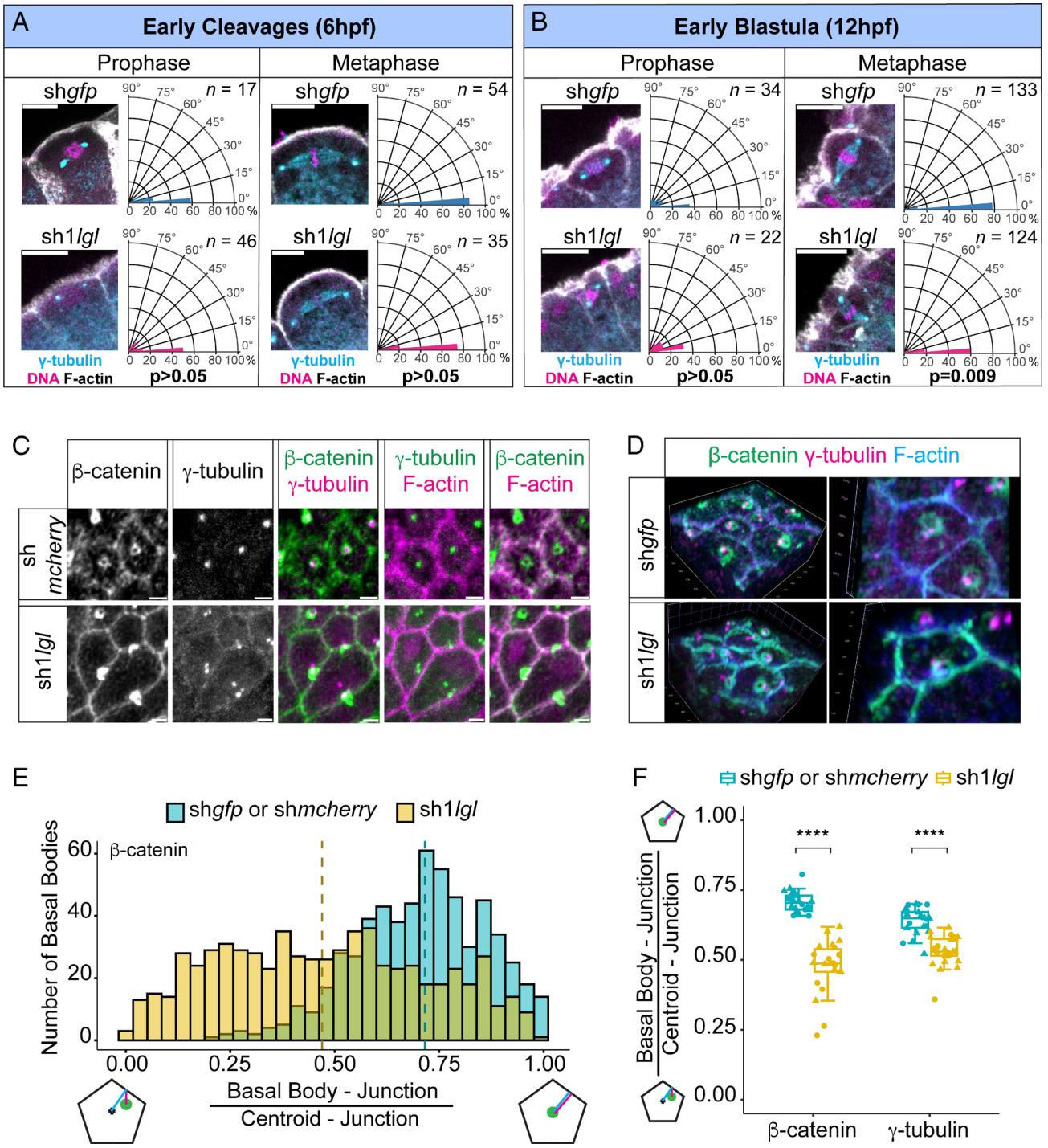


**Fig. 4.** Centrosomes and basal bodies are mispositioned in *lgl* knockdown ectodermal epithelia. (*A* and *B*) Prophase and metaphase spindles identified by γ-tubulin enrichment at the spindle centrosomes in sh*gfp* control and sh1*lgl* embryos during early cleavage and blastula stages. Corresponding fan plots show the percentage of spindles that are parallel (angle: 0 degrees) or perpendicular to the plane of the ectodermal epithelium (angle: 90 degrees). Prophase spindles show a randomized orientation relative to the epithelial plane in both sh*gfp* and sh1*lgl* embryos. Metaphase spindles align with the plane of the epithelium in sh*gfp* embryos. However, in sh1*lgl* embryos, a significant percentage of spindles deviates from the epithelial plane during early blastula cleavages shown in (*B*). (Wilcoxon rank sum test; $P = 0.009$). *n* indicates the number of spindles. Number of sh*gfp* embryos analyzed per time point: 6hpf (10 embryos) and 12hpf (25 embryos). Number of sh*lgl* embryos analyzed per time point: 6hpf (12 embryos) and 12hpf (21 embryos). With the exception of 12hpf metaphase spindles, the median angle of spindle orientation is not significantly different between sh*gpf* and sh1*lgl* embryos (Wilcoxon rank sum test; $P > 0.05$). (*C*) Position of the basal body in sh*gfp* control and sh1*lgl* embryos as indicated by the enrichment of β-catenin and γ-tubulin relative to the junctions of ectodermal epithelial cells. (*D*) Closeup 3D projection views of β-catenin enrichment near the basal body as indicated by enrichment of γ-tubulin in sh*gfp* and sh1*lgl* embryos. Basal bodies are near-center-localized in sh*gfp* controls and closer to the cell junctions in sh1*lgl* embryos. (*E*) Distribution of basal body positions relative to the cell center and cell junction in sh*gfp* control and sh1*lgl* embryos. Medians are 0.716 for sh*gfp* and 0.47 for sh1*lgl* basal bodies. Analysis was based on β-catenin-marked basal bodies and cell junctions. (*F*) Average ratios of β-catenin and γ-tubulin-marked basal body positions relative to the cell center and cell junction in sh*gfp* control and sh1*lgl* embryos. Symbols ▲● correspond to ratios from two independent experiments. Ratio = 1 indicates basal body position closer to the center of the cell. Ratio < 0.5 indicates basal body position closer to the cell junction. Number of β-catenin-marked-basal bodies analyzed in 20 sh*gfp* embryos: 601. Number of β-catenin-marked-basal bodies analyzed in 22 sh1*lgl* embryos: 661. Number of γ-tubulin-marked-basal bodies analyzed in 22 sh*gfp* embryos: 660. Number of γ-tubulin-marked-basal bodies analyzed in 26 sh1*lgl* embryos: 780. (Wilcoxon rank sum test; ****$P < 0.0001$). Images and quantifications are from postgastrula embryos. Scale bars in A and B: 10 μm and in C: 2 μm.

## Discussion

Epithelia are the first organized tissues to appear during animal development (1). Epithelia emerge as cells divide, differentiate, and migrate to form distinct territories and organs. *Nematostella* embryos self-organize into epithelial layers early during development and provide an excellent system for studying epithelial organization in isolation, independent of the confounding effects of signaling from neighboring organs and tissues (11, 20). Additionally, dissociated *Nematostella* embryonic cells self-organize into a complete animal after aggregation (12). We reasoned that epithelialization of aggregates requires the conserved polarity proteins necessary to form epithelia in other animals. We found that aggregates from *Nematostella* cells with reduced expression of the lateral polarity protein Lgl failed to organize within a common epithelial outer layer and they eventually disintegrated. This striking result first confirms that successful epithelialization needs to occur before an aggregate can further develop into an animal. Second, lateral cell polarization is essential for aggregate epithelialization. Adhesion of cells is not sufficient to hold the sh*lgl* aggregate together. In the absence of an outer epithelial layer, sh*lgl* cells come together in rosette-like clusters which eventually disintegrate and do not coalesce into building a common tissue/animal. Is lateral polarity *only* required for de novo epithelialization of aggregates? We found that *lgl* knockdown also impaired embryonic epithelia. It is likely that embryos lacking expression of Lgl are structurally compromised and their dissociation gives rise to cells that lack the potential to epithelialize. A future experiment would be to trigger expression of Lgl in dissociated cells postaggregation and examine whether its presence restores epithelialization. Taken together, loss of lateral polarity is detrimental for both embryonic and aggregate epithelialization.

Indeed, embryos with reduced *lgl* expression develop surface depressions that accompany basal polarity defects. Specifically, we found three features that perturb the basal domain of the ectodermal monolayer. First, round nonmitotic cells occupy the basal domain. This is in contrast to normal epithelia, where mitotic cells undergo cortical rounding exclusively in the apical domain and no round cells appear in the basal domain (30). Second, some cells develop apical character in the basal region of the ectodermal epithelium. Interestingly, GFP fusions to Par3 and Par6 localized normally to apical domains in *lgl* knockdown embryos, indicating normal apical polarity even when epithelia were highly disorganized. In normal epithelia, apical proteins are not encountered in the basal domain. Studies in bilaterians have uncovered a robust mechanism that blocks apical proteins from localizing to the basal domain of epithelial cells (2, 6). Although not yet examined in *Nematostella*, Lgl may play a direct or indirect role in apical protein exclusion from the basal domain. Finally, basal junctions were not confined in the basal domain of the monolayer. Instead, we found both α-catenin-GFP and phosphorylated myosin localized at various lengths from the apical domain. This could be due to mis-localization of basal junctional proteins along normally elongated epithelial cells. Alternatively, the cells develop basal polarity but are shorter in length. Together, these three features help explain the formation of a bilayered structure composed of basal cells with reversed polarity to that of the apical cells stacked above them.

A mechanism that could give rise to basal cells with reverse polarity is misoriented cell division. When mitotic spindles are positioned in oblique or orthogonal angles relative to the epithelial plane, one of the daughter cells ends up in the basal domain of the monolayer. If one daughter cell polarizes in mirror symmetry to the other, we would expect to find cells with their apical proteins in the basal domain and their basal proteins buried within the monolayer. We did find a higher number of misoriented cleavages in *lgl* knockdown embryos during early blastula. Few misoriented cell divisions early during development could strongly impact epithelial organization.

We were surprised to find that although the apical domains of *lgl* knockdown epithelia were properly polarized, basal bodies of their cilia were mispositioned. Depending on the phase of the cell cycle, centrioles organize into spindle poles during mitosis and basal bodies during interphase (33). In normal epithelia, basal bodies are anchored within close range to the centroid of the apical domain. In *lgl* knockdown embryos, we observed a high proportion of basal bodies positioned very close to the lateral plasma membrane. Disruption of cytoskeletal organization is likely to impair basal body migration or docking to the apical cell membrane. A similar defect and basal body anchoring to the lateral plasma membrane was observed when quail oviducts were treated with Benzodiazepines. These drug treatments impair cortical actomyosin and vesicle trafficking, suggesting that basal body mispositioning is due to a migration defect (34). Misorientation of the mitotic spindle during early blastula cell divisions and mispositioning of the basal body in interphase cells of *lgl* knockdown embryos, both point to a potential centriole movement defect.

It is unclear whether Lgl has a direct role on centriole positioning in *Nematostella* epithelia. In human embryonic kidney cells, Lgl2 binds and regulates the localization of Pins (Partner of Inscutable) which has a role in spindle pole orientation (35). Lgl is also implicated in the regulation of symmetric cell divisions in fly epithelia (36, 37). However, in fly, it is cortical release of Lgl that drives proper cell division. Retention of Lgl on the cortex impairs spindle positioning. Lgl cortical release frees Dlg to interact with Pins in the lateral domain and promote planar orientation of the spindle. Moreover, *lgl* mutant follicular epithelial cells and syncytial embryos assemble normal spindles and undergo normal chromosome segregation respectively, suggesting that in the fly Lgl does not have a direct role in chromosome segregation (36). Other factors, such as well-organized cortical actomyosin is critical for planar spindle orientation in epithelial tissues and could also play a role in *Nematostella* embryos.

We propose that in *Nematostella*, the lateral polarity protein Lgl is important for epithelialization mainly through its effect on the organization of the cytoskeleton. Cell shape change, misorientation of the mitotic spindle, and mispositioning of the ciliary basal body in *lgl* knockdown embryos could be all attributed to a failure of cytoskeletal organization. Early studies in *Drosophila* showed that Lgl binds to and regulates the localization of myosin II (38, 39). Cells in *lgl* knockdown embryos and imaginal discs are cuboidal or round instead of long and columnar and as a result fail to establish extended lateral contacts. It was proposed that the Lgl–myosin complex stabilizes newly formed lateral cell contacts and maintains cell shape (38, 40). Human Lgl also binds to myosin II, and in *lgl* knockout mice brains, the organization of actin and localization of myosin II are perturbed (27, 41).

Interestingly, we did not find any correlation between Lgl and cell proliferation control in early *Nematostella* embryos. Since its discovery as a tumor suppressor in the fly, Lgl has been shown to be important for control of cell proliferation in various organs including imaginal discs, brain, eye, and egg chamber (22, 23, 42–44). In mammals, Lgl affects cell numbers in the brains of mouse embryos and human mammary epithelial cells grown in a 3-dimensional extracellular matrix (27, 45). However, in some of these cases, cell division is coupled to tissue differentiation. For example, knockout of one of the two Lgl homologs in mice (Lgl1)

leads to loss of asymmetric inheritance of the Notch signaling antagonist Numb, and neural progenitors fail to differentiate and instead proliferate into tumor-like structures (27). It will be important to examine the effect of *lgl* expression later during *Nematostella* development, when cells are undergoing differentiation and organ development.

Epithelialization is a fundamental tissue organization process that occurs in all developing animals. However, it is context dependent with variations across animals, tissues within animals and stages of development (1, 2). In search of conserved principles that underly metazoan epithelialization, we find that lateral polarity is essential for the organization of epithelial layers during both embryonic development and aggregate organization. Among the many factors that are at play during epithelialization, our results support an important role for lateral polarization. In the absence of defined lateral polarity, adhesion proteins are not sufficient to organize cells into an epithelium. Similarly, in some in vitro experiments, cysts developing in suspension from Madin Darby Canine Kidney (MDCK) cells require the formation of both lateral cell contacts and basal lamina during epithelialization (46). The establishment of lateral polarity may be a central feature of epithelial organization in other developmental contexts. In many animals including some sponges, snails, and annelids, epithelia emerge from a solid ball of cells, the stereoblastula (47). Lateral polarization in these embryos may facilitate cell layer organization during gastrulation. Accordingly, we speculate that lateral polarization may have facilitated the evolution of epithelia in solid cell aggregates and in contexts where cleavages were not constrained to organize cells into monolayers. Finally, it is intriguing that knockdown of Lgl alone led to a dramatic epithelialization defect in both embryonic and aggregate epithelia without an obvious effect on embryo cell proliferation. The impact of *lgl* knockdown on cell shape and organelle localization in both *Nematostella* and fly epithelia point to the conserved role of Lgl in the organization of the cytoskeleton. This finding generates questions on the molecular evolution of Lgl in its control of both epithelial organization and cell proliferation encountered in different systems.

## Materials and Methods

Animal culture and embryo handling were as previously described (48). Genes were knocked down by electroporation and microinjection of in vitro synthesized shRNAs as described in ref. 49. Embryos were dissociated and reaggregated according to ref. 12. Extensive descriptions of all procedures, including embryo manipulations, immunohistochemistry, imaging, and image analysis are included in the *Materials and Methods* of *SI Appendix, Supporting Information*.

**Data, Materials, and Software Availability.** All study data are included in the article and/or supporting information.

**ACKNOWLEDGMENTS.** We are grateful to Dr Lampros Panagis (Amherst Biology Imaging Center) and Phillip Zhou for training and help with imaging, Dr Nicholas Horton and Clara Page for advice on statistical analysis, Dr Cheng-Yi Chen for qPCR advice, and Caroline Towse and the Biology Department of Amherst College for animal maintenance and administrative assistance. Our work is supported by Amherst College, a NSF Grant MRI-2117798 and a National Institute of General Medical Sciences Grant R15GM141979-01.

1. S. Doerr, P. Zhou, K. Ragkousi, Origin and development of primary animal epithelia. *BioEssays* **46**, 2300150 (2024).
2. C. E. Buckley, D. St Johnston, Apical–basal polarity and the control of epithelial form and function. *Nat. Rev. Mol. Cell Biol.* **23**, 559–577 (2022).
3. C. R. Magie, M. Q. Martindale, Cell-cell adhesion in the Cnidaria: Insights into the evolution of tissue morphogenesis. *Biol. Bull.* **214**, 218–232 (2008).
4. S. P. Leys, A. Riesgo, Epithelia, an evolutionary novelty of metazoans. *J. Exp. Zool. B Mol. Dev. Evol.* **318**, 438–447 (2012).
5. P. W. Miller, D. N. Clarke, W. I. Weis, C. J. Lowe, W. J. Nelson, The evolutionary origin of epithelial cell–cell adhesion mechanisms. *Curr. Top. Membr.* **72**, 267–311 (2013).
6. E. Rodriguez-Boulan, I. G. Macara, Organization and execution of the epithelial polarity programme. *Nat. Rev. Mol. Cell Biol.* **15**, 225–242 (2014).
7. N. H. Putnam *et al.*, Sea anemone genome reveals ancestral eumetazoan gene repertoire and genomic organization. *Science* **317**, 86–94 (2007).
8. B. Zimmermann *et al.*, Topological structures and syntenic conservation in sea anemone genomes. *Nat. Commun.* **14**, 8270 (2023).
9. E. A. Pukhlyakova, A. O. Kirillova, Y. A. Kraus, B. Zimmermann, U. Technau, A cadherin switch marks germ layer formation in the diploblastic sea anemone *Nematostella vectensis*. *Development* **146**, dev174623 (2019).
10. D. N. Clarke, C. J. Lowe, W. James Nelson, The cadherin-catenin complex is necessary for cell adhesion and embryogenesis in *Nematostella vectensis*. *Dev. Biol.* **447**, 170–181 (2019).
11. J. H. Fritzenwanker, G. Genikhovich, Y. Kraus, U. Technau, Early development and axis specification in the sea anemone *Nematostella vectensis*. *Dev. Biol.* **310**, 264–279 (2007).
12. A. Kirillova *et al.*, Germ-layer commitment and axis formation in sea anemone embryonic cell aggregates. *Proc. Natl. Acad. Sci. U.S.A.* **115**, 1813–1818 (2018).
13. G. Giudice, Restitution of whole larvae from disaggregated cells of sea urchin embryos. *Dev. Biol.* **5**, 402–411 (1962).
14. A. Gierer *et al.*, Regeneration of *Hydra* from reaggregated cells. *Nat. New Biol.* **239**, 98–101 (1972).
15. M. Dan-Sohkawa, H. Yamanaka, K. Watanabe, Reconstruction of bipinnaria larvae from dissociated embryonic cells of the starfish, Asterina pectinifera. *Development* **94**, 47–60 (1986).
16. S. H. Bernacki, D. R. McClay, Embryonic cellular organization: Differential restriction of fates as revealed by cell aggregates and lineage markers. *J. Exp. Zool.* **251**, 203–216 (1989).
17. T. D. Skokan, R. D. Vale, K. L. McKinley, Cell sorting in *Hydra vulgaris* arises from differing capacities for epithelialization between cell types. *Curr. Biol.* **30**, 3713–3723.e3 (2020).
18. R. A. Foty, M. S. Steinberg, The differential adhesion hypothesis: A direct evaluation. *Dev. Biol.* **278**, 255–263 (2005).
19. G. W. Brodland, The Differential Interfacial Tension Hypothesis (DITH): A comprehensive theory for the self-rearrangement of embryonic cells and tissues. *J. Biomech. Eng.* **124**, 188–197 (2002).
20. K. Ragkousi, K. Marr, S. McKinney, L. Ellington, M. C. Gibson, Cell-cycle-coupled oscillations in apical polarity and intercellular contact maintain order in embryonic epithelia. *Curr. Biol.* **27**, 1381–1386 (2017).
21. M. Salinas-Saavedra, T. Q. Stephenson, C. W. Dunn, M. Q. Martindale, Par system components are asymmetrically localized in ectodermal epithelia, but not during early development in the sea anemone *Nematostella vectensis*. *Evodevo* **6**, 20 (2015).
22. E. Gateff, Malignant neoplasms of genetic origin in *Drosophila melanogaster*. *Science* **200**, 1448–1459 (1978).
23. D. Bilder, M. Li, N. Perrimon, Cooperative regulation of cell polarity and growth by *Drosophila* tumor suppressors. *Science* **289**, 113–116 (2000).
24. M. L. Heuzé *et al.*, Myosin II isoforms play distinct roles in adherens junction biogenesis. *Elife* **8**, e46599 (2019).
25. G. Tanentzapf, U. Tepass, Interactions between the *crumbs*, *lethal giant larvae* and *bazooka* pathways in epithelial polarization. *Nat. Cell Biol.* **5**, 46–52 (2003).
26. E. Gateff, H. A. Schneiderman, Developmental capacities of benign and malignant neoplasms of *Drosophila*. *Wilhelm Roux Arch. Entwickl. Mech. Org.* **176**, 23–65 (1974).
27. O. Klezovitch, T. E. Fernandez, S. J. Tapscott, V. Vasioukhin, Loss of cell polarity causes severe brain dysplasia in Lgl1 knockout mice. *Genes Dev.* **18**, 559–571 (2004).
28. F. di Pietro, A. Echard, X. Morin, Regulation of mitotic spindle orientation: An integrated view. *EMBO Rep.* **17**, 1106–1130 (2016).
29. X. Morin, Y. Bellaïche, Mitotic spindle orientation in asymmetric and symmetric cell divisions during animal development. *Dev. Cell* **21**, 102–119 (2011).
30. K. Ragkousi, M. C. Gibson, Cell division and the maintenance of epithelial order. *J. Cell Biol.* **207**, 181–188 (2014).
31. D. T. Bergstralh, T. Haack, D. St Johnston, Epithelial polarity and spindle orientation: Intersecting pathways. *Philos. Trans. R Soc. B Biol. Sci.* **368**, 20130291 (2013).
32. Y. Nakajima, Mitotic spindle orientation in epithelial homeostasis and plasticity. *J. Biochem.* **164**, 277–284 (2018).
33. T. Kobayashi, B. D. Dynlacht, Regulating the transition from centriole to basal body. *J. Cell Biol.* **193**, 435–444 (2011).
34. E. Boisvieux-Ulrich, M.-C. Laine, D. Sandoz, *In vitro* effects of benzodiazepines on ciliogenesis in the quail oviduct. *Cell Motil.* **8**, 333–344 (1987).
35. M. Yasumi *et al.*, Direct binding of Lgl2 to LGN during mitosis and its requirement for normal cell division. *J. Biol. Chem.* **280**, 6761–6765 (2005).
36. C. A. Carvalho, S. Moreira, G. Ventura, C. E. Sunkel, E. Morais-De-Sá, Aurora A triggers Lgl cortical release during symmetric division to control planar spindle orientation. *Curr. Biol.* **25**, 53–60 (2015).
37. G. P. Bell, G. C. Fletcher, R. Brain, B. J. Thompson, Aurora kinases phosphorylate Lgl to induce mitotic spindle orientation in *Drosophila* epithelia. *Curr. Biol.* **25**, 61–68 (2015).
38. D. Strand, I. Raska, B. M. Mechler, The *Drosophila lethal(2)giant larvae* tumor suppressor protein is a component of the cytoskeleton. *J. Cell Biol.* **127**, 1345–1360 (1994).
39. D. Strand *et al.*, The *Drosophila lethal(2)giant larvae* tumor suppressor protein forms homo-oligomers and is associated with nonmuscle myosin II heavy chain. *J. Cell Biol.* **127**, 1361–1373 (1994).
40. P. Manfruelli, N. Arquier, W. P. Hanratty, M. Sémériva, The tumor suppressor gene, *lethal(2)giant larvae (l(2)gl)*, is required for cell shape change of epithelial cells during *Drosophila* development. *Development* **122**, 2283–2294 (1996).
41. D. Strand *et al.*, A human homologue of the *Drosophila* tumour suppressor gene *l(2)gl* maps to 17p11.2–12 and codes for a cytoskeletal protein that associates with nonmuscle myosin II heavy chain. *Oncogene* **11**, 291–301 (1995).

42. F. Wirtz-Peitz, T. Nishimura, J. A. Knoblich, Linking cell cycle to asymmetric division: Aurora-A phosphorylates the Par complex to regulate Numb localization. *Cell* **135**, 161–173 (2008).
43. N. A. Grzeschik, N. Amin, J. Secombe, A. M. Brumby, H. E. Richardson, Abnormalities in cell proliferation and apico-basal cell polarity are separable in Drosophila *lgl* mutant clones in the developing eye. *Dev. Biol.* **311**, 106–123 (2007).
44. M. Zhao, P. Szafranski, C. A. Hall, S. Goode, Basolateral junctions utilize Warts signaling to control epithelial–mesenchymal transition and proliferation crucial for migration and invasion of *Drosophila* ovarian epithelial cells. *Genetics* **178**, 1947–1971 (2008).
45. A. Russ, J. M. V. Louderbough, D. Zarnescu, J. A. Schroeder, Hugl1 and Hugl2 in mammary epithelial cells: Polarity, proliferation, and differentiation. *PLoS One* **7**, e47734 (2012).
46. A. Z. Wang, G. K. Ojakian, W. J. Nelson, Steps in the morphogenesis of a polarized epithelium: I. uncoupling the roles of cell–cell and cell-substratum contact in establishing plasma membrane polarity in multicellular epithelial (MDCK) cysts. *J. Cell Sci.* **95**, 137–151 (1990).
47. S. F. Brusca, G.J. BruscaR.C. Gilbert, "Characteristics of metazoan development" in *Embryology: Constructing the Organism*, A. M. Gilbert, S.F. Raunio, Ed. (1997), pp. 3–19.
48. J. H. Fritzenwanker, U. Technau, Induction of gametogenesis in the basal cnidarian *Nematostella vectensis* (Anthozoa). *Dev. Genes. Evol.* **212**, 99–103 (2002).
49. A. Karabulut, S. He, C.-Y. Chen, S. A. McKinney, M. C. Gibson, Electroporation of short hairpin RNAs for rapid and efficient gene knockdown in the starlet sea anemone. Nematostella vectensis. *Dev. Biol.* **448**, 7–15 (2019).